J Electroceram (2007) 19:243–250
DOI 10.1007/s10832-007-9058-x

Magnetoelectric interactions in ferromagnetic-piezoelectric layered structures: Phenomena and devices

M. I. Bichurin · D. Viehland · G. Srinivasan

Received: 11 April 2006 / Accepted: 21 August 2006 / Published online: 28 February 2007

Abstract Layered magnetostrictive-piezoelectric structures are multifunctional due to their dual-responsiveness to mechanical and electromagnetic forces. Here, we discuss studies of magnetoelectric (ME) interactions in ferrite-lead zirconate titanate (PZT) and terfenol-PZT material couples. Key findings include: (1) the observation of a giant low-frequency ME effect in the layered systems; (2) data analysis based on our model for low frequency ME effects; (3) observation and theory of enhanced ME coupling at the electromechanical resonance (EMR); and (4) theory and measurements of microwave ME effects, at the ferromagnetic resonance of ferrites. The layered structures are potential candidates for sensors, gyrators and microwave devices. Low frequency sensors are feasible with excellent sensitivity to minute magnetic field variations. One could also realize composite based ferromagnetic resonance devices, such as resonators, filters and phase shifters with electric field tunability for use at 1–70 GHz.

Keywords Magnetoelectric effect · Sensor · Gyrator · Filter · Phase shifter

M. I. Bichurin (✉)
Institute of Electronic and Informative Systems,
Novgorod State University,
173003 Veliky Novgorod, Russia
e-mail: bmi@mail.natm.ru

D. Viehland
Materials Science and Engineering, Virginia Tech,
Blacksburg, VA 24061, USA

G. Srinivasan
Physics Department, Oakland University,
Rochester, MI 48309, USA

1 Introduction

A multiferroic is a material that exhibits two or more primary ferroic properties (i.e., ferromagnetism, ferroelectricity, ferroelasticity). Such dual-responsiveness could also be realized in a composite material. For example, a composite of ferromagnetic and ferroelectric materials allows coupling between magnetization and polarization; and is therefore a magnetoelectric (ME) multiferroic. The ME coupling between the piezoelectric and magnetostrictive phases is mediated via mechanical forces.

The ME effect is defined as the dielectric polarization response of a material to an applied magnetic field, or an induced magnetization change upon application of an external electric field [1, 2]. The induced polarization P is related to the magnetic field H by the expression, $P=\alpha H$, where α is the second rank ME-susceptibility tensor. The (static) effect was first observed in antiferromagnetic Cr_2O_3 But most single phase compounds show only weak ME interactions [3]. However, composites of piezomagnetic-piezoelectric phases are also magnetoelectric. When said composites are subjected to a bias magnetic field H, a magnetostriction induced strain is coupled to the ferroelectric phase that results in an induced electric field E via piezoelectricity. The ME susceptibility, $\alpha=\delta P/\delta H$, is the product of the piezomagnetic deformation $\delta l/\delta H$ and the piezoelectric charge generation $\delta P/\delta l$ [1]. Here, in this paper, we are primarily interested in the dynamic ME effect. For an ac magnetic field δH applied to a biased laminate composite, one measures the induced voltage δV. The ME voltage coefficient $\alpha_E=\delta V/t\ \delta H$ (or $\alpha=\varepsilon_o\varepsilon_r\alpha_E$), where t is the composite thickness and ε_r is the relative permittivity. These composites product tensor-property offer (1) the opportunity for studies on the physics of ME

coupling, and (2) enormous potential for novel devices that would allow E and H control of electromagnetic properties.

2 Low-frequency magnetoelectric effects: experiment and theory

In order to obtain high ME couplings, a layered structure must be insulating, in order that it can be poled to align the electric dipole moments [3–6]. To achieve these requirements, Harshe proposed laminate structures, provided a theoretical model for bilayer laminates, and reported weak ME coupling in multilayers of CFO-PZT or $BaTiO_3$ [3]. Recently, we have succeeded in achieving giant ME effects, close to that theoretically predicted, in ferrite/PZT laminate composites by choosing ferrites with high piezomagnetic coupling [8, 9] and terfenol-D/PZT laminates [7].

2.1 Giant low frequency ME effects in ferrite-PZT and ferromagnetic metal-PZT

We reported strong magnetoelectric (ME) couplings in layered composites of nickel ferrite-PZT and nickel zinc ferrite-PZT [8, 9]. Samples of ferrites and PZT prepared were made by tape-casting thick layers. Thin disks of sintered multilayers were poled by an electric field applied perpendicularly to its plane. For ME studies, these laminates were polished, electrical contacts were made with silver paint, and subsequently poled. The poling procedure involved heating the sample to 420 K, and re-cooling to 300 K under an electric field of E=20–50 kV/cm. The samples were then positioned in a shielded three-terminal sample holder and placed between the pole pieces of an electromagnet (0–18 kOe) used for applying a magnetic bias field H. The required ac magnetic field δH=1 Oe at 10 Hz–10 kHz applied parallel to H was generated with a pair of Helmholtz coils. The ac electric field δE perpendicular to the sample plane was estimated from the voltage δV measured by a lock-in-amplifier. The ME coefficient α_E was measured for three conditions: (1) transverse or $\alpha_{E,31}$ for H and δH parallel to each other and to the disk plane (1,2) and perpendicular to δE (direction-3), (2) longitudinal or $\alpha_{E,33}$ for all the three fields parallel to each other and perpendicular to sample plane and (3) in-plane $\alpha_{E,11}$ for all the three fields parallel to each other and parallel to sample plane. Figure 1 shows representative data on H dependence of α_E at 300 K and 100 Hz for nickel zinc ferrite (NZFO) and PZT [8, 9]. An increase in α_E with H to a maximum value is observed, followed by a rapid drop. The coefficients are directly proportional to the piezomagnetic coupling $q=\delta\lambda/\delta H$, where λ is the magnetostriction, and the H-dependence tracks the slope of λ vs H. Saturation of λ at high field leads to α_E=0. The transverse coefficient is much higher than the longitudinal values due to the absence of demagnetization effects. Further, the strong piezomagnetic coefficient for in-plane magnetic fields is the cause of giant transverse ME coefficients.

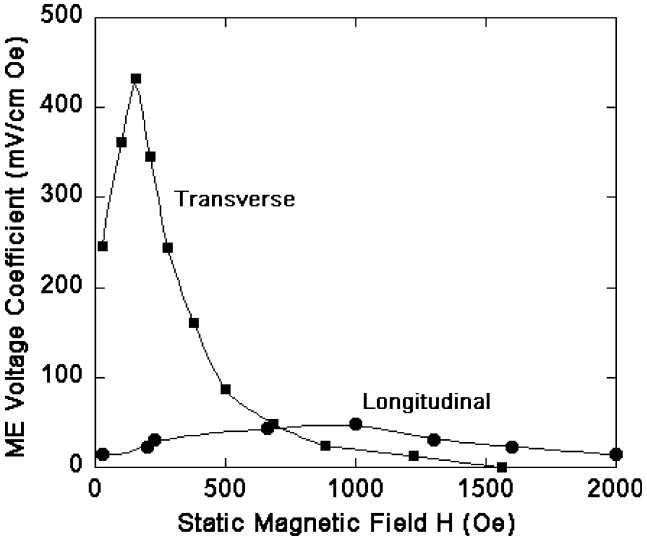

Fig. 1 Transverse and longitudinal ME voltage coefficients versus H at 100 Hz for a multilayer sample with 21 layers of nickel zinc ferrite, $Ni_{0.8}Zn_{0.2}Fe_2O_4$, and 20 layers of PZT and a layer thickness of 20 μm

A model was developed for low-frequency ME effects in bilayers of magnetostrictive and piezoelectric phases [10]. A novel approach, the introduction of an interface coupling parameter k, was proposed for the consideration of actual boundary conditions at the interface. An averaging method was used to estimate effective material parameters. The theory predicted a giant ME coupling for ferrite-PZT and terfenol-D/PZT, in agreement with measured values.

The following expressions were obtained for the ME coefficients [10]

$$\alpha_{E,33}=\frac{E_3}{H_3}=2\frac{\mu_0 v(1-v)^p d_{31}{}^m q_{31}}{\{2^p d_{31}^2(1-v)+{}^p\varepsilon_{33}[({}^ps_{11}+{}^ps_{12})(v-1)-v({}^ms_{11}+{}^ms_{12})]\}}\times \times\frac{[({}^ps_{11}+{}^ps_{12})(v-1)-v({}^ms_{11}+{}^ms_{12})]}{\{[\mu_0(v-1)-{}^m\mu_{33}v][v({}^ms_{12}+{}^ms_{11})-({}^ps_{11}+{}^ps_{12})(v-1)]+2^m q_{31}^2 v^2\}} \quad (1)$$

$$\alpha_{E,31}=\frac{E_3}{H_1}=\frac{-v(1-v)({}^mq_{11}+{}^mq_{21})^p d_{31}}{{}^p\varepsilon_{33}({}^ms_{12}+{}^ms_{11})v+{}^p\varepsilon_{33}({}^ps_{11}+{}^ps_{12})(1-v)-2^p d_{31}^2(1-v)}$$

Here ${}^ps_{ij}$ and ${}^pd_{ki}$ are compliance and piezoelectric coefficients, and ${}^p\varepsilon_{kn}$ is the permittivity matrix, $\boldsymbol{H}_k$ and $\boldsymbol{E}_k$ are the vector components of magnetic and electric fields, ${}^mq_{ki}$ and ${}^m\mu_{kn}$ are piezomagnetic coefficients and the permeability matrix, v is the PZT volume fraction. Estimated values based on Eq. 1 and data were in good agreement [7–9].

2.2 Interactions at electromechanical resonance

An ME phenomenon of fundamental and technological interests is an enhancement in the coupling, when the electrical or magnetic sub-system undergoes resonance: i.e., electromechanical resonance (EMR) for PZT and ferromagnetic resonance (FMR) for the ferrite. Previously, we reported on these effects and provided theoretical models. The resonance ME effect is similar in nature to a standard one, i.e., an induced polarization under the action of an ac magnetic field: but, the ac field here is tuned to the electromechanical resonance frequency. As the dynamic magnetostriction is responsible for the electromagnetic coupling, EMR leads to significant increasing in the ME voltage coefficients [11, 12]. Measurements of resonance ME effects were carried out on composites of ferrite, terfenol-D or transition metal, and PZT. The data in Fig. 2 for a trilayer of Ni-PZT-Ni shows a 2–3 orders of magnitude increase in $\alpha_{E,31}$ at EMR due to radial modes compared to low frequency values. We developed the theory for ME coupling at EMR for a ferromagnetic/piezoelectric bilayer [11].

2.3 Resonance ME effects at FMR

Previously, we reported microwave ME interactions by studies of ferromagnetic resonance (FMR) in bilayers of single crystal ferromagnetic-piezoelectric oxides [13], and also developed theoretical models for the effects [14, 15]. An electric field E produces a mechanical deformation in the piezoelectric phase, resulting in a shift in the resonance field for the ferromagnet. Figure 3 shows the estimated resonance profiles with and without electric fields for bilayers of nickel ferrite-PZT, lithium ferrite-PZT, and yttrium iron garnet-PZT. The results predict the highest resonance field shift for NFO-PZT, and the smallest for YIG-PZT. The strength of the ME coupling at resonance was obtained from data on the resonance field shift vs. E in bi-layers of YIG films and (001) lead magnesium niobate-lead titanate (PMN-PT). Figure 4 shows data for such field shift versus E, and one infers a stronger ME coupling in thinner YIG films. The ME phenomenon at microwave

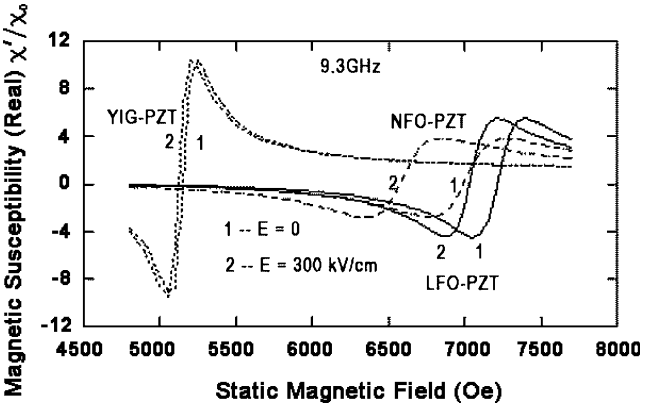

Fig. 3 Theoretical static magnetic field H dependence of the magnetic susceptibility for a bilayer of ferrite-lead titanate zirconate (PZT). The results are for lithium ferrite (LFO)-PZT, nickel ferrite (NFO)-PZT, and yttrium iron garnet (YIG)-PZT bilayers. The susceptibility at 9.3 GHz are for H and E perpendicular to sample plane and for electric fields of (1) E=0 and (2) E=300 kV/cm. Notice the down-shift in the resonance field when E is increased from 0 to 300 kV/cm

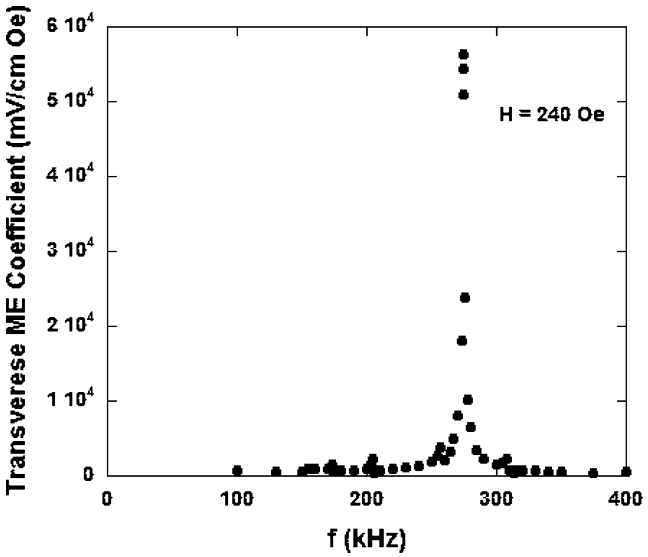

Fig. 2 ME coupling at electromechanical resonance (*EMR*) due to radial modes in a 9 mm diameter trilayer of Ni-PZT-Ni. The thickness of each layer is 0.4 mm

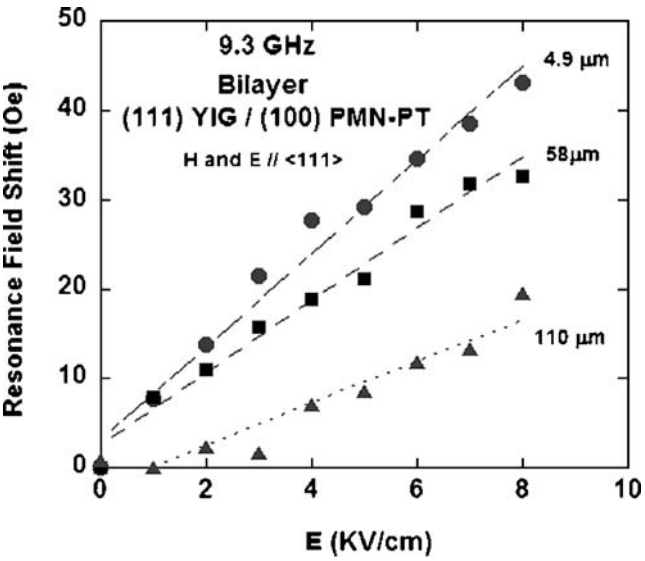

Fig. 4 Microwave magnetoelectric effect at 9.3 GHz in bilayers of (111) YIG on GGG and (100) PMN-PT. The static fields E and H are parallel to <111> of YIG and is perpendicular to the bilayer plane. The shift in the resonance field δH_E, measured from FMR profiles as a function of E for a series of YIG film thickness. The *lines* are linear fit to the data

frequencies are important for the realization of *electric field tunable* microwave phase shifters and band-pass filters.

2.4 ME effects at magneto-acoustic resonance

The third resonance phenomenon of importance is the ME interactions at the coincidence of the FMR and EMR, at magnetoacoustic resonance (MAR). At the FMR, spin-lattice coupling and spin waves that couple energy to phonons through relaxation processes are expected to enhance the piezoelectric and ME interactions. Further strengthening of the ME coupling is expected at the overlap of FMR and EMR. We developed a model for the effect [16]. Figure 5 provides theoretical estimates on the variation of the ME voltage coefficient α_E with frequency of the ac magnetic field applied to a bilayer of NFO-PZT. The thickness of NFO and PZT layers are 100 and 200 nm, respectively. In (a) the bias field H_0 is smaller than the field H_r for FMR in NFO. The peaks in α_E occur at the fundamental and second harmonic of the EMR for the thickness modes of the bilayer. In (b): H_o is selected so that FMR in NFO coincides with the fundamental EMR mode, resulting in the enhancement in α_E at the MAR. In (c) the second harmonic of acoustic modes in NFO-PZT coincides with FMR. Thus one observes a dramatic increase in α_E at MAR.

Significant results and implications of our model are as follows: (1) Coincidence of the FMR and EMR allows energy transfer between phonons, spin waves and electric and magnetic fields. This transformation is found to be very efficient in ferrite-PZT; (2) ultrahigh ME coefficients are predicted at MAR; and (3) the effect is important for miniature/nanosensors and transducers at microwave frequencies.

2.5 ME interactions in nano-discs and nano-walls

Nanowires, nanotubes, nanorods, etc. constitute an important class of one-dimensional (1D) nanostructures that are presently a subject of very active investigation. These structures are ideally suited to study the interrelationship between electrical, transport, optical and other functional properties that exhibit dimensional and size restrictions. Inorganic nanowires have already been demonstrated as components for a host of exciting applications in nano-electronics, including FETs, logic gates and single electron transistors, and optoelectronic devices. Furthermore, their high stiffness and strength lend them to applications as nanoscale actuators, force sensors and calorimeters. Because of the large surface areas of 1D nanostructures, a more effective interface coupling between the layers in a multiferroic composite is to be expected that would likely lead to an enhancement in the ME effect. However, a fundamental understanding of the size and shape-dependent scaling behavior of the ME effect in composites, particularly down to nanoscale dimensions, is presently lacking. An improved knowledge of the nanoscale ME properties will help achieve miniaturization of magnetoelectric devices. The properties of magnetic nanowires have been studied in some detail recently and their scaling properties with reduced dimensions are reasonably well understood,

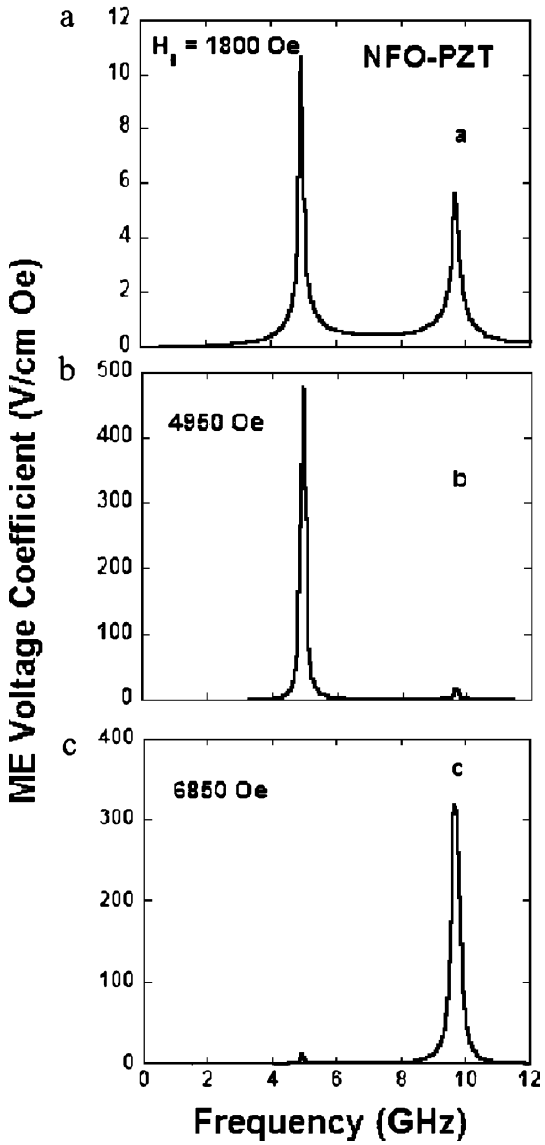

Fig. 5 Theoretical estimates on the variation of magnetoelectric (ME) voltage coefficient α_E with the frequency of ac magnetic field for a bilayer of nickel ferrite (NFO)-lead zirconate titanate (PZT). The thickness of NFO and PZT layers are 100 nm and 200 nm, respectively. **a** The bias field H_0 is smaller than the field H_r for ferromagnetic resonance (*FMR*) in NFO. The peaks in α_E occur at the fundamental and second harmonic in electromechanical resonance (*EMR*) for thickness modes for the bilayer. **b** The ME coupling at the coincidence of EMR and FMR, the magneto-acoustic resonance (*MAR*). H_o is selected so that FMR in NFO coincides with the fundamental EMR mode, resulting in the enhancement in α_E at MAR. **c** Similar result as in **b**, but for MAR at the second harmonic of acoustic modes in NFO-PZT

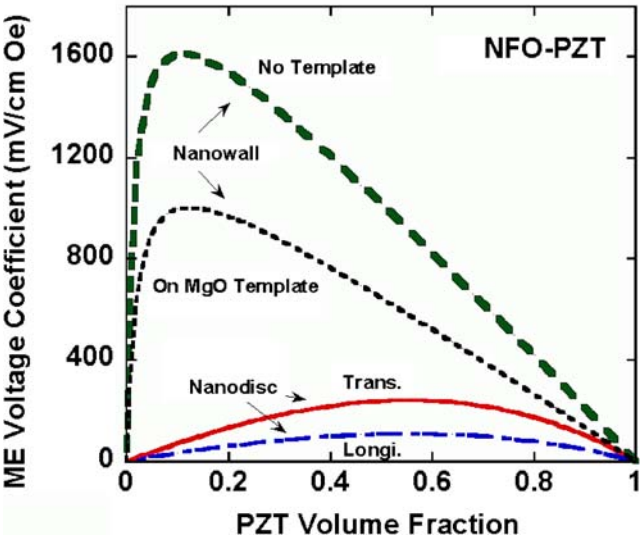

Fig. 6 PZT volume fraction dependence of ME voltage coefficient for NFO-PZT nano-disc on MgO and nano-tube with MgO template (for Radius of MgO stub = half of the nano-tube) and without a template

particularly for those based on magnetic transition metals and their alloys. In contrast, there has been limited work on the ferroelectric properties of 1 D structures. This is in large part because of the difficulties associated with the synthesis of materials with complex chemical structures.

We have extended our low-frequency ME model for some representative nanostructures. Figure 6 provides estimates on ME voltage coefficients for a series of NFO-PZT nano-composites and important results are summarized below.

In nanodiscs on MgO, the strength of ME interactions is weaker than thick film bilayers due to clamping effects of the MgO substrate. For the nanodisc, the ME effect for transverse ME voltage coefficient exceeds the longitudinal coefficient because of demagnetization fields. For the nanowall (Fig. 7), the MgO template reduces the strength of ME effect (as in the case of nanodiscs). Increasing the MgO template radius decreases the ME effect. Comparison of the ME effect in nano-tube and nano-plate shows that in

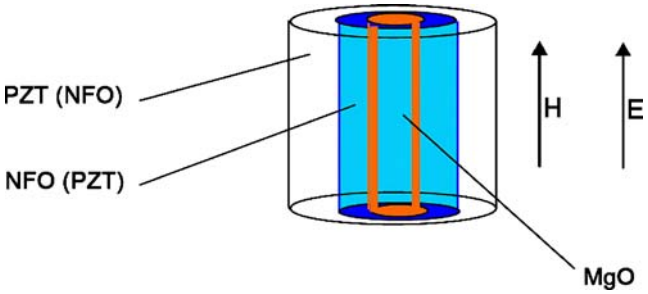

Fig. 7 Proposed nanowalls on MgO template

the first case the radial stress is added to in-plane stresses. This results in strong ME effect.

3 Magnetoelectric devices

One of the most important components of our efforts is the fabrication of low frequency and microwave devices with the use of the composites. Efforts to date focused on (1) sensors [17], (2) gyrators [18, 19], (3) filters [21] and (4) phase shifters based on ME effects in composites [20]. Most ferrite-based devices use a permanent magnet to generate the bias field. The frequency tuning, therefore, is rather slow and involves high power. With a ME composite, however, fast frequency tuning could be accomplished with an easy to generate electric field.

3.1 ME magnetic field sensor

We have mitigated the low frequency thermal-noise limitations [17] by developing identical piezoelectric layers which are (1) mechanically disconnected; (2) thermally connected (i.e., packaged together); and (3) electrically connected in reverse. An example of said approach is providing in Fig. 8a, which illustrates a push–pull laminate configuration. For this configuration, thermal noise acts on small neighboring elements similarly; consequently, any temperature changes

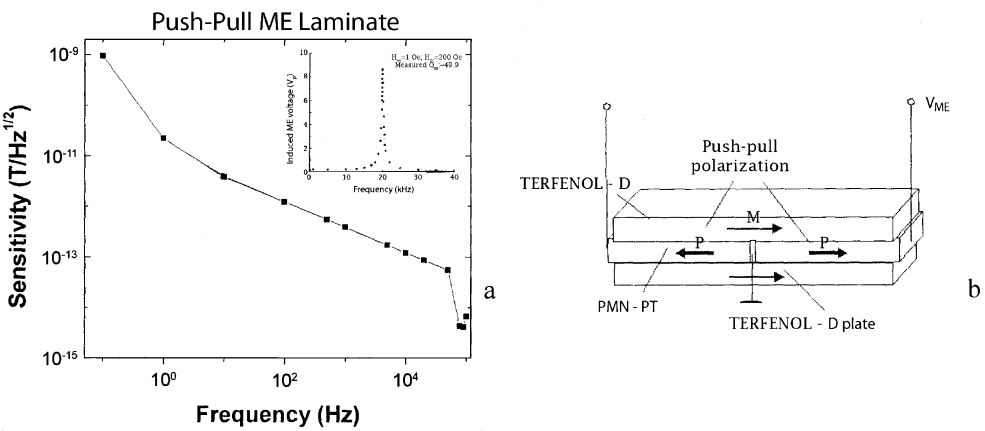

Fig. 8 **a** Noise spectra, given in Tesla/Hz$^{1/2}$, for the push–pull ME laminate. These data were taken at 300 K; and **b** Schematic view of our magneto-electric push-pull laminate composite magnetic field sensors

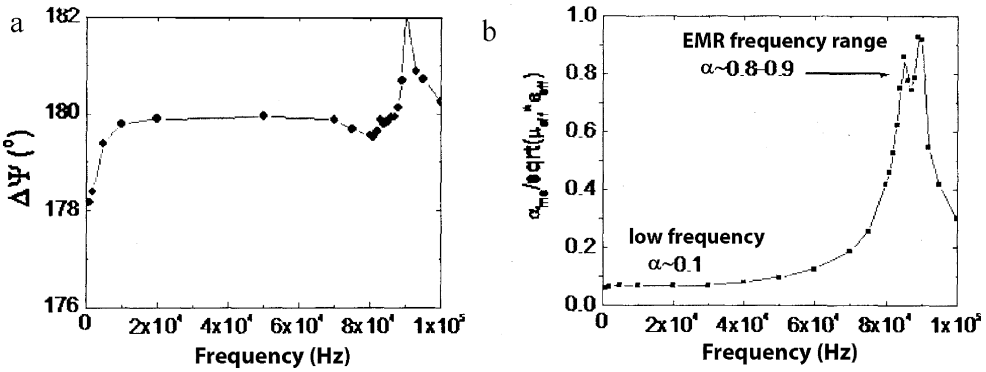

Fig. 9 Gyrator characteristics of ME laminate composite. **a** 180° phase shift between I and V, fulfillment of criterion 1. **b** Large gyration near EMR, fulfillment of criterion 2

generate an equal and compensating charge in the mechanically disconnected layer, resulting in enhanced noise rejection. In Part (b) of this figure, we present the noise spectra. Data are shown over a frequency range of $0.1<f<10^5$ Hz. The low frequency data were taken using a high-resistance input op-amp, whereas the high frequency data were taken by a voltage method. At 1 Hz, the sensitivity limit to minute magnetic field variations was about 3×10^{-11} T/Hz$^{1/2}$ (RMS), and its noise-equivalent charge on the order of 10^{-15} C. With increasing frequency, the noise floor was dramatically lowered, reaching about 2×10^{-15} T/Hz (RMS) at the resonance frequency of the laminate (~10^5 Hz).

3.2 ME gyrator

An ideal gyrator must meet two existence criteria, as originally given by Tellegen [19]. First, it must obey the following set of linear algebraic equations

$$V_1 = -\alpha I_2;\ V_2 = \alpha I_1, \tag{2}$$

where V is voltage, I is current, and α is a conversion (or gyration) coefficient between voltage and current. Non-reciprocity is manifested as an 180° phase difference between α in the first and the second rows. Second, to qualify as an 'ideal' gyrator, his material must meet the following criteria

$$\frac{\alpha_{me}c_0}{\sqrt{\mu_{eff}\varepsilon_{eff}}} \approx 1, \tag{3}$$

where α_{me} is the magnetoelectric susceptibility, c_{o} is the speed of light in vacuum, $\varepsilon_{\mathrm{eff}}$ is the effective relative dielectric constant, and μ_{eff} is the effective relative permeability. Only when conditions 2 and 3 are simultaneously satisfied can complete and total conversion between I and V, or vice-versa, occur.

We have discovered [18] that laminated composites of piezoelectric (PZT) and magnetostrictive (Terfenol-D) layers can come close to meeting these two criteria for ideal gyrators at EMR range. In Fig. 9 we illustrate the frequency dependence of gyrator characteristics for transverse mode in trilayer structure Terfenol-D-PZT-Terfenol-D. Data presented in Fig. 9 and checking its operation as impedance inverter show that we got the near ideal gyrator at EMR range.

3.3 ME filter

An electric field tunable microwave band-pass filter based on ferromagnetic resonance (FMR) in a bilayer of YIG and PZT has been designed and characterized. The filter tunability is accomplished through magnetoelectric (ME) coupling that manifests as a shift in the FMR. Studies on a microstripline filter show a 125-MHz tuning range for E= 0–3 kV/cm and an insertion loss of 5 dB at 6.5 GHz.

The single-cavity ME filter, shown in Fig. 10, consists of a 1 mm thick dielectric ground plane (permittivity of 10), input and output microstrips of non-resonance lengths, and an ME-element [21]. The input–output decoupling is

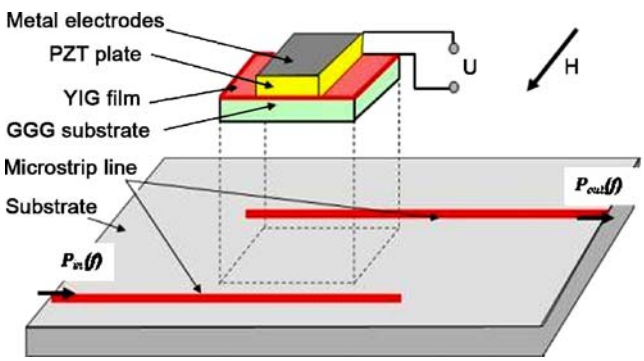

Fig. 10 Diagram showing a microwave ME filter

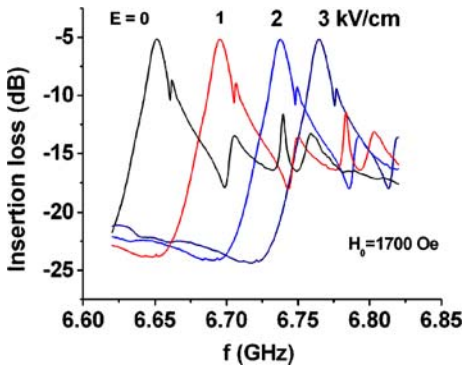

Fig. 11 The transmission characteristics for ME microwave filter

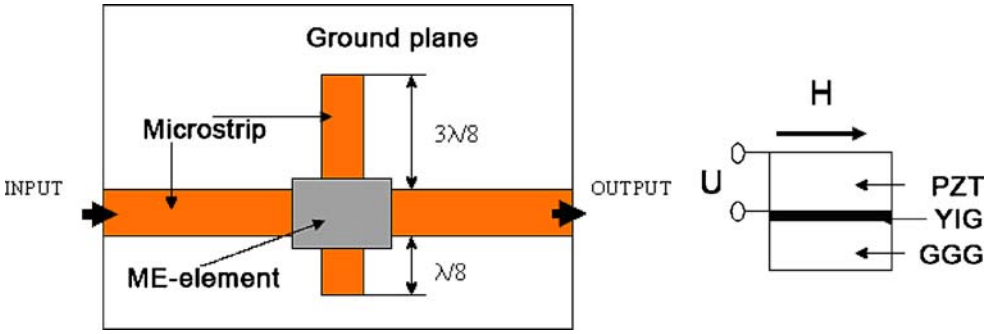

Fig. 12 A magnetoelectric microwave phase shifter

determined by the gap between the microstrips. In our device, the microstrip transducers, 1 mm in width and 18 mm in length, are separated by 2.5 mm. Power is coupled from input to output under FMR in the ME element. The ME element consisted of epitaxial YIG film bonded to PZT. A 110 μm thick YIG film grown by liquid-phase epitaxy on a (111) gadolinium gallium garnet was used. The film had the dimensions 5.5×1.5 mm^2, saturation induction 4 πM of 1750 G, and FMR line-width of 1 Oe. A PZT plate with the dimensions 4×1×0.5 mm^3 was initially poled by heating up to 150°C and cooling back to room temperature in an electric field of 10 kV/cm perpendicular to the sample plane. The layered structure was made by bonding the YIG film surface to PZT with 0.08 mm thick layer of ethyl cyanoacrylate, a fast-dry epoxy. The layered structure was placed between of the transducers as in Fig. 10 and was subjected to a field H parallel to the sample plane and perpendicular to the microstrips.

The device characterization was carried out with a vector network analyzer (PNA E-8361). An input continuous-wave signal $P_{in}(f)$=1 mW was applied to the filter. The frequency f dependence of the insertion loss L, i.e., the transmitted power through the ME element, was measured at 4–10 GHz as a function of H and E applied across the PZT layer. Representative results on L vs. f are shown in Fig. 11. Consider first the profile for E=0. The maximum input–output coupling is observed at f_r=6.77 GHz that corresponds to FMR in YIG for an in-plane H=1.7 kOe, 4 πM=1.75 kG and gyromagnetic ratio γ=2.8 GHz/kOe. The loss increases sharply $f<f_r$ and the off-resonance isolation is 20–25 dB. For $f>f_r$, secondary maxima due to magnetostatic modes are seen in Fig. 11. A significant modification of L vs. f profile is observed in Fig. 11 when E=1 kV/cm is applied across PZT; f_r is down-shifted by δf= 28 MHz. The shift arises due to strain at YIG-PZT interface caused by the piezoelectric deformation in PZT. Further increase in E results in increase in the magnitude of the down-shift as shown in Fig. 11. We observed an up-shift in f_r when the direction of E was reversed by reversing the polarity of applied voltage and is attributed to a switch from compressive to tensile strain in YIG. Thus, a microwave magnetoelectric based on YIG/PZT layered structure has been designed and characterized. The filter can be tuned by 2% of the central frequency with a nominal electric field of 3 kV/cm.

3.4 ME phase shifter

An electric field tunable YIG-PZT phase shifter based on ferromagnetic resonance (FMR) is designed and characterized. The electric field control of the phase shift $\delta\phi$ arises through magnetoelectric interactions. The piezoelectric deformation in PZT in an electric field E leads to a shift in the FMR frequency in YIG and a phase shift. For E=5–8 kV/cm applied across PZT, $\delta\phi$=90–180° and an insertion loss of 1.5–4 dB are obtained. Theoretical estimates of δϕ are in excellent agreement with the data.

The design for the ME microwave phase shifter is shown in Fig. 12 [20]. It consists of a 1 mm wide microstrip on a 1 mm thick aluminum oxide ground plane (relative permittivity of 10), a YIG-PZT resonator and microstrip loops of length $\lambda/8$ and $3\lambda/8$ that produce a circularly polarized microwave magnetic field in the resonator. The ME resonator consisted of a 0.5 mm thick, 5 mm×5 mm plate of PZT and a 4 mm×2.5 mm epitaxial (100) YIG film of thickness 124 μm on 0.5 mm thick gadolinium gallium garnet (GGG) substrate. Silver electrodes were deposited on

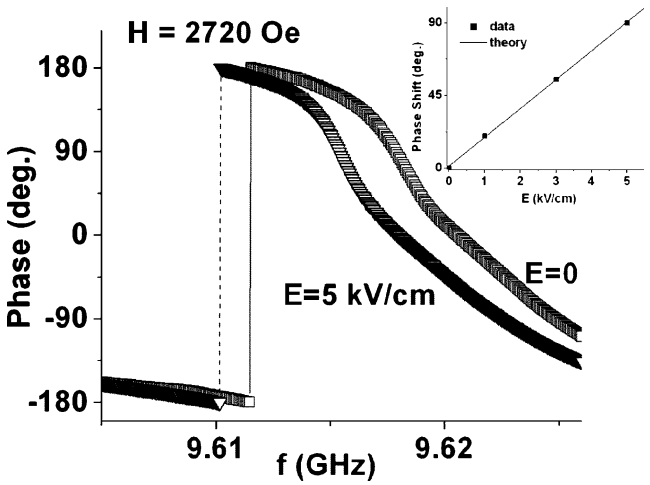

Fig. 13 Frequency dependence of phase characteristics for ME microwave phase shifter

PZT that was poled by heating up to 150°C and cooling back to room temperature in an electric field of 20 kV/cm perpendicular to the sample plane. The YIG film with saturation magnetization of 1,750 Oe and FMR line-width of 1 Oe was bonded to PZT with a 0.08 mm thick layer of ethyl cyanoacrylate, a fast-dry epoxy.

The device characteristics were studied with a vector network analyzer (Agilent PNA E-8361). An input cw signal $P_{in}(f)$ of frequency f=1–10 GHz and power P_{in}= −10 dBm was applied to the input transducer. The frequency dependences of the insertion loss $L(f)=20 \log [P_{out}(f)/P_{in}(f)]$ and phase shift $\varphi(f)$ of the output signal were measured as a function of H_o and E. Representative data on the electric field tunable YIG-PZT phase shifters are shown in Fig. 13 for H_0=2,720 Oe, a bias field corresponding to a linear variation of μ' with H. The frequency shift for E= 5 kV/cm is 2 MHz, and one observes a linear variation in $\delta\varphi$ with E.

4 Conclusions

Studies on layered samples of ferrites-PZT show evidence for strong ME interactions. Of particular interest is the giant ME voltage coefficients in nickel ferrite-PZT and terfenol-D/PZT. An order of magnitude enhancement in the strength of ME interactions was measured at electromechanical resonance in nickel ferrite-PZT and terfenol-D/PZT layered samples. The phenomenon could be utilized to accomplish very high field conversion efficiency in the product property composites. We have designed novel low frequency ME devices such as magnetic field sensors and gyrators that possess by unique parameters. Microwave magnetoelectric coupling has been studied through FMR at 9.3 GHz in (111)YIG/(001)PMN-PT bilayers. The results have been used to design and estimate the performance characteristics of an electric field tunable YIG/PMNPT filter and phase-shifter. Insertion loss as low as 1.1 dB are expected for a filter consisting of ME resonators. For nominal electric fields of 100 kV/cm, the filter was tuned over a frequency band of 1.4 GHz and the phase shifter by a phase angle about 360°. The electric tuning would facilitate high-speed operation, small size and compatibility with integrated circuit technology.

Acknowledgements The work at Oakland University and Virginia Tech. was supported by grants from the National Science Foundation, the Office of Naval Research and the Army Research Office. The work at Novgorod State University was supported by the Russian Foundation for Basic Research (projects No. 06-08-00896-a, 06-02-08071-ofi and 05-02-39002-GFEN-a).

References

1. J. Van Suchtelen, Philips Res. Rep. **27**, 28 (1972)
2. J. van den Boomgaard, A.M.J.G. van Run, J. van Suchtelen, Ferroelectrics **14**, 727 (1976)
3. G. Harshe, *Magnetoelectric effect in piezoelectric-magnetostrictive composites*, PhD thesis. (The Pennsylvania State University, College Park, PA, 1991)
4. T.G. Lupeiko, I.V. Lisnevskaya, M.D. Chkheidze, B.I. Zvyagintsev, Inorg. Mater. **31**, 1245 (1995)
5. J.G. Wan, J.-M. Liu, H.L.W. Chand, C.L. Choy, G.H. Wang, C.W. Nan, J. Appl. Phys. **93**, 9916 (2003)
6. J. Ryu, A.V. Carazo, K. Uchino, H. Kim, Jpn. J. Appl. Phys. **40**, 4948 (2001)
7. S. Dong, J.F. Li, D. Viehland, Appl. Phys. Lett. **83**, 2265 (2003); IEEE Trans. Ultrason. Ferroelectr. Freq. Control **50**, 10 (2003)
8. G. Srinivasan, E.T. Rasmussen, J. Gallegos, R. Srinivasan, Yu. I. Bokhan, V.M. Laletin, Phys. Rev., B **64**, 214408 (2001)
9. G. Srinivasan, E.T. Rasmussen, R. Hayes, Phys. Rev., B **67**, 014418 (2003)
10. M.I. Bichurin, V.M. Petrov, G. Srinivasan, Phys. Rev., B **68**, 054402 (2003)
11. M.I. Bichurin, D.A. Fillipov, V.M. Petrov, U. Laletsin, G. Srinivasan, Phys. Rev., B **68**, 132408 (2003)
12. S. Dong, J. Cheng, J.F. Li, D. Viehland, Appl. Phys. Lett. **83**, 4812 (2003)
13. S. Shastry, G. Srinivasan, M.I. Bichurin,V.M. Petrov, A.S. Tatarenko, Phys. Rev., B **70**, 064416 (2004)
14. M.I. Bichurin, V.M. Petrov, I.A. Kornev, A.S. Tatarenko, Yu. V. Kiliba, G. Srinivasan, Phys. Rev., B **68**, 054402 (2003)
15. M.I. Bichurin, V.M. Petrov, Yu. V. Kiliba, G. Srinivasan, Phys. Rev., B **66**, 134404 (2002)
16. M.I. Bichurin, V.M. Petrov, O.A. Ryabkov, S.V. Averkin, G. Srinivasan, Phys. Rev., B **72**, 060408(R) (2005)
17. Junyi Zhai, Z. Xing, S. Dong, J.F. Li, D. Viehland, Appl. Phys. Lett. **88**, 062510-1 (2006)
18. Junyi Zhai, Jiefang Li, Shuxiang Dong, D. Viehland, M.I. Bichurin, J. Appl. Phys. **100**, 124509 (2006)
19. B.D.H. Tellegen, Philips Res. Rep. **3**, 81 (1948)
20. M.I. Bichurin, R.V. Petrov, Yu. V. Kiliba, Ferroelectrics **204**, 311 (1997)
21. G. Srinivasan, A.S. Tatarenko, M.I. Bichurin, Electron. Lett. **41**, 596 (2005)